AIMS Electronic Research Archive

https://www.aimspress.com/journal/era

ERA, 34(9): 6432–6447.
DOI: 10.3934/era.2026281
Received: 06 May 2026
Revised: 25 June 2026
Accepted: 07 July 2026
Published: 20 July 2026

Research article

Robust data-driven control for set-point tracking of linear discrete-time systems with time delays

Chengyan Wang, Xingren Chen and Shi Li*

School of Electrical and Automation Engineering, Nanjing Normal University, Nanjing 210046, China

* **Correspondence:** Email: lishilln@njnu.edu.cn.

Abstract: This paper focused on the direct data-driven set-point tracking control problem of linear discrete-time systems with input time-delay. First, a tracking error was introduced by constructing an extended state vector through state reconstruction to generate a data-driven model. Second, a data-based tracking controller was designed with the objective of minimizing the L_2 gain from disturbances to the performance output through H_∞ control, thereby reducing the impact of input delay and disturbance and ensuring asymptotic tracking stability. Finally, to validate the effectiveness and practicality of the proposed method, this paper took an autonomous direct current (DC) micro-grid with two distributed generation units as the research object. Through simulation results, the effectiveness of the data-driven method in addressing set-point tracking control issues for time-delay systems was demonstrated.

Keywords: data-driven control; set-point tracking; input time-delay; H_∞ control

1. Introduction

In the industrial sector, traditional modeling methods based on first principles or recognition face numerous challenges. As production technologies advance, actual processes become increasingly complex, significantly increasing the difficulty of modeling. Additionally, traditional model-based control (MBC) theory [1] struggles to model dynamic and complex systems, resulting in poor safety and robustness. However, modern industrial processes generate vast amounts of data containing valuable information. Against this backdrop, data-driven control (DDC) has emerged [2]. DDC eliminates the reliance on precise models, effectively addressing the system's nonlinearity, time-varying characteristics, and uncertainty, while also being easy to implement. Therefore, in the development of control theory and technology, the transition from traditional model-based control methods to DDC methods has become an important research direction.

DDC, as an interdisciplinary field bridging data science and control engineering, originated from breakthroughs in computer science. The rapid development of various learning methods, such as reinforcement learning [3] and vehicle control [4], has provided control systems with novel data processing and decision-making approaches. However, robust controllers are essential for ensuring system stability. Consequently, the field of DDC has recently shifted its focus toward developing controller synthesis methods rooted in traditional control strategies. In recent years, this approach has yielded significant research results in the field of linear system control. Scholars typically assume that the underlying system follows linear dynamic characteristics and use this as a basis for analyzing collected data. Additionally, they fully consider practical factors such as noise interference to construct a DDC framework capable of achieving robust control. Recent research outcomes include data-driven predictive control [5–7], piecewise affine systems [8], state feedback and optimal control [9–12], among others.

In the field of automatic control, tracking control occupies a central position [13, 14]. Its core objective is to design control laws that drive the output or state of the controlled system to precisely and robustly follow a predefined desired trajectory or set-point. However, achieving high-performance tracking control presents numerous challenges, including system model uncertainty, unknown external disturbances, and time delays, all of which can significantly impact tracking accuracy and complicate system dynamics. To address these challenges, researchers have drawn inspiration from classical control theory [15, 16], modern control theory [17, 18], and DDC methods such as linear quadratic tracking (LQT) [19] to develop systematic design frameworks.

On the other hand, research on time-delay systems (TDS) poses certain challenges for data-driven methods. Unlike constant delays, time-varying delays introduce dynamic uncertainty, significantly complicating stability analysis and requiring controllers to adapt to time-varying parameter changes. Although MBC methods [20, 21] for time-varying delays are relatively mature, their corresponding data-driven methods remain underdeveloped. Many data-driven strategies for systems with time delays assume that the delay is known or fixed [22, 23], thereby limiting their applicability to systems with unknown, complex, or time-varying delay patterns. Compared with the above studies, [9] demonstrated achievable performance under uncertain or rapidly varying delays. This result extends the applicability of data-driven control to a broader class of delay systems and motivates the present work.

To the best of the authors' knowledge, data-driven tracking control subject to uncertain input delays and disturbances has rarely been studied. Inspired by [9] and [19], we focus on the research of DDC based on set-point tracking in linear discrete-time (LDT) systems with input delays. Specifically, the following contributions are derived:

(1) Different from [5, 8, 11] where the data-driven stabilization problems were studied, this paper focuses on a more complex data-driven tracking control problem. We introduce tracking error as a state variable, expand the initial state equation, and collect state data and input data for the new state equation.

(2) Based on the collected input and state data, this paper designs a data-driven tracking controller based on H_∞ control. In this case, uncertain input delays and disturbances are considered, which reduces the impact of the input delay and disturbance and ensures asymptotic tracking stability.

Notations: Let $\mathbb{Z}$ and $\mathbb{Z}^+$ denote the sets of integers and positive integers, respectively. $\mathbb{R}$ is the set of real numbers, and $\mathbb{R}^{m\times n}$ denotes the set of all real matrices of dimension $m \times n$. The superscripts X^T and X^{-1} indicate the transpose and inverse of a matrix, respectively. The appropriate identity matrix is presented by I. $\star$ represents the transpose of the corresponding matrix. For any matrix B, $\bar{B} = \bar{\mathcal{P}}_2 B \bar{\mathcal{P}}_2$.

Table 1. Summary of key symbols used in the equations.

Symbol	Description
$d(s)$	Time-varying input delay at sampling time s
$\bar{d}$	Known upper bound of the delay $d(s)$
$e(s)$	Set-point tracking error, $e(s) = y(s) - \theta(s)$
K	Number of recorded data samples
γ	Disturbance attenuation level (L_2-gain bound)
η	Tuning parameter introduced via $\mathcal{P}_3 = \eta\mathcal{P}_2$
$\mathcal{K}$	Feedback gain matrix
Q_1, Q_2	Auxiliary data-based decision matrices
n, m, q	Dimensions of the state, input, and output
W_0	Combined open-loop data matrix

2. Problem analysis and preparation

Consider the LDT-TDS:

$$\begin{cases} x(s+1) = Ax(s) + Bu_{d(s)}(s) + Dw(s) \\ \quad y(s) = Cx(s), \end{cases} \tag{2.1}$$

where $x(s) \in \mathbb{R}^n$ is the system state; $u_{d(s)}(s) \in \mathbb{R}^m$ is the control input with delay $d(s)$; $w(s) \in \mathbb{R}^p$ is the system disturbance; $y(s) \in \mathbb{R}^q$ is the controlled output; s represents the sampling time. Matrices $A \in \mathbb{R}^{n\times n}$, $B \in \mathbb{R}^{n\times m}$, and $C \in \mathbb{R}^{q\times n}$ are unknown. $D \in \mathbb{R}^{n\times p}$ is known.

Remark 1. *For the system, $d(s) \in \{0, 1, \ldots, \bar{d}\}$ for $s \in \mathbb{Z}^+$, $u_{d(s)}(s) := u(s - d(s))$.*

Assumption 1. *Controllability holds for the pair (A, B), and observability holds for the pair (A, C).*

The reference signal for multi-output set-point tracking is given by a specified constant matrix $\theta = \begin{bmatrix}\theta_1 & \cdots & \theta_q\end{bmatrix}^\top \in \mathbb{R}^q$. For consistency,

$$\theta(s) = \theta. \tag{2.2}$$

Remark 2. *This paper aims to develop a DDC controller to achieve reference signal tracking, ensuring the set point tracking error $e(s) = y(s) - \theta(s)$ converges to zero as $s \to \infty$.*

Combining Eqs (2.1) and (2.2), define $\mathfrak{X}(s) = \begin{bmatrix}\Delta x(s)^\top & e(s)^\top\end{bmatrix}^\top$, $\Delta x(s) = x(s+1) - x(s)$, $\mathcal{W}(s) = \Delta w(s) = w(s+1) - w(s)$, $\mathcal{U}_{d(s)}(s) = u_{d(s+1)}(s+1) - u_{d(s)}(s)$. For $e(s+1) = e(s) + \Delta e(s) = e(s) + C\Delta x(s)$, and we can obtain

$$\mathfrak{X}(s+1) = \mathcal{A}\mathfrak{X}(s) + \mathcal{B}\mathcal{U}_{d(s)}(s) + \mathcal{D}\mathcal{W}(s), \tag{2.3}$$

where

$$\mathcal{A} = \begin{bmatrix} A & 0 \\ C & I_q \end{bmatrix}, \mathcal{B} = \begin{bmatrix} B \\ 0 \end{bmatrix}, \mathcal{D} = \begin{bmatrix} D \\ 0 \end{bmatrix}.$$

Setting $\mathcal{K} = [\mathcal{K}_1 \quad \mathcal{K}_2]$ with $\mathcal{K} \in \mathbb{R}^{m\times(n+q)}$, we can get

$$\mathcal{U}(s) = \mathcal{K}\mathfrak{X}(s) = \mathcal{K}_1\Delta x(s) + \mathcal{K}_2 e(s). \tag{2.4}$$

By summing both sides of Eq (2.4) from 0 to $s-1$, we obtain

$$u(s) = u(0) + \mathcal{K}_1(x(s) - x(0)) + \mathcal{K}_2 \sum_{i=0}^{s-1} e(i). \tag{2.5}$$

System (2.3) can be rewritten as

$$\mathfrak{X}(s+1) = \begin{bmatrix} \mathcal{B} & \mathcal{A} \end{bmatrix} \begin{bmatrix} \mathcal{U}_{d(s)}(s) \\ \mathfrak{X}(s) \end{bmatrix} + \mathcal{D}\mathcal{W}(s). \tag{2.6}$$

The system data is sampled at discrete time instants and stacked into the following matrix form:

$$\begin{aligned}
\mathfrak{X}_{\{0\}} &:= \begin{bmatrix} \mathfrak{X}(0) & \mathfrak{X}(1) & \dots & \mathfrak{X}(K-1) \end{bmatrix}, \\
\mathcal{U}_{d,\{0\}} &:= \begin{bmatrix} \mathcal{U}(0-d(0)) & \mathcal{U}(1-d(1)) & \dots & \mathcal{U}(K-1-d(K-1)) \end{bmatrix}, \\
\mathfrak{X}_{\{1\}} &:= \begin{bmatrix} \mathfrak{X}(1) & \mathfrak{X}(2) & \dots & \mathfrak{X}(K) \end{bmatrix},
\end{aligned}$$

where $K \in \mathbb{Z}$ represents the sample size and $\mathcal{U}_{d,\{0\}} \in \mathbb{R}^{m\times K}$, $\mathfrak{X}_{\{0\}} \in \mathbb{R}^{(n+q)\times K}$, $\mathfrak{X}_{\{1\}} \in \mathbb{R}^{(n+q)\times K}$.

Problem 1. *Consider system* (2.3) *with a given delay bound* $\bar{d} > 0$*. For a feedback gain* $\mathcal{K}$*, we can obtain the following closed-loop system under* $\mathcal{U}(s) = \mathcal{K}\mathfrak{X}(s)$

$$\mathfrak{X}(s+1) = \mathcal{A}\mathfrak{X}(s) + \mathcal{B}\mathcal{K}\mathfrak{X}_{d(s)}(s) + \mathcal{D}\mathcal{W}(s), \tag{2.7}$$

with the given performance output

$$Z(s) = L\mathfrak{X}(s), \tag{2.8}$$

where $Z(s) \in \mathbb{R}^q$ *and constant matrices* $L \in \mathbb{R}^{q\times(n+q)}$*. In this case, given a fixed value of* $\gamma > 0$*, for* $d(s) \in [0, \bar{d}]$*, this paper aims to obtain a feedback gain* $\mathcal{K}$ *such that system* (2.7) *is asymptotically stable when* $\mathcal{W}(s) = 0$*; system* (2.7) *achieves an* L_2*-gain below* γ *when* $\mathcal{W}(s) \neq 0$.

The following assumptions underpin this analysis.

Assumption 2.

(1) *$\mathcal{A}$ and $\mathcal{B}$ are constant but unknown matrices.*
(2) *The upper bound of the input delay $\bar{d} \in \mathbb{Z}_{>0}$ is known.*
(3) *$\mathcal{U}_{d,\{0\}}$, $\mathfrak{X}_{\{0\}}$, and $\mathfrak{X}_{\{1\}}$ are available, where $K \in \mathbb{Z}_{>0}$ represents the number of recorded samples.*

Remark 3. *The data collection process is carried out under open-loop conditions, with the control input generated by a random excitation signal rather than by closed-loop feedback. This avoids the high correlation among state variables that can arise in closed-loop systems due to the feedback mechanism. Open-loop random excitation can independently explore different directions of the state space, thereby ensuring that the data matrix* W_0 *satisfies the required rank condition* $\mathrm{rank}(W_0) = m + n + q$*. If data collection must be performed under closed-loop conditions, an additional excitation signal would need to be superimposed to break the state correlation introduced by feedback.*

Considering the above assumptions, representing the system solely by data, let

$$W_0 := \begin{bmatrix} \mathcal{U}_{d,\{0\}} \\ \mathfrak{X}_{\{0\}} \end{bmatrix} \in \mathbb{R}^{(m+n+q)\times K}. \tag{2.9}$$

The open-loop database is represented as

$$\mathfrak{X}(s+1) = \mathfrak{X}_{\{1\}} W_0^{\dagger} \begin{bmatrix} \mathcal{U}_{d(s)}(s) \\ \mathfrak{X}(s) \end{bmatrix} + \mathcal{D}\mathcal{W}(s). \tag{2.10}$$

It is easy to verify that the system trajectories of (2.10) are equivalent to the ones of (2.3) if W_0 satisfies $\operatorname{rank}(W_0) = m+n+q$ [9]. Meanwhile, $\begin{bmatrix} \mathcal{B} & \mathcal{A} \end{bmatrix} = \mathfrak{X}_{\{1\}} W_0^{\dagger}$.

Consider system (2.3) and assume $\mathcal{U}_{d(s)}(s) = \mathcal{K}\mathfrak{X}_{d(s)}(s)$. It is easy to obtain

$$\mathfrak{X}(s+1) = \begin{bmatrix} \mathcal{B}\mathcal{K} & \mathcal{A} \end{bmatrix} \begin{bmatrix} \mathfrak{X}_{d(s)}(s) \\ \mathfrak{X}(s) \end{bmatrix} + \mathcal{D}\mathcal{W}(s), \tag{2.11}$$

and

$$\mathfrak{X}(s+1) = \mathfrak{X}_{\{1\}} H_K \begin{bmatrix} \mathfrak{X}_{d(s)}(s) \\ \mathfrak{X}(s) \end{bmatrix} + \mathcal{D}\mathcal{W}(s), \tag{2.12}$$

where H_K is a $K \times 2(n+q)$ matrix which satisfies

$$\begin{bmatrix} \mathcal{K} & 0 \\ 0 & I_{n+q} \end{bmatrix} = W_0 H_K \tag{2.13}$$

and

$$\mathcal{U}_{d(s)}(s) = \mathcal{U}_{d,\{0\}} H_K \begin{bmatrix} I_{n+q} & 0 \end{bmatrix}^{\top} \mathfrak{X}(s). \tag{2.14}$$

3. Data-driven stabilization

Theorem 1. *Given positive constants $\bar{d}$, γ and the tuning parameter η, if there exist matrices $\bar{\mathcal{P}} > 0$, $\bar{\mathcal{G}} > 0$, $\bar{\mathcal{R}} > 0$, $\bar{\mathcal{G}}_{12} > 0$, and matrices Q_1, Q_2 with appropriate dimensions guaranteeing the fulfillment of the following data-based inequality constraints:*

$$\bar{\Gamma} > 0, \tag{3.1}$$

$$\begin{bmatrix} \bar{\mathcal{R}} & \bar{\mathcal{G}}_{12} \\ \star & \bar{\mathcal{R}} \end{bmatrix} \geq 0, \tag{3.2}$$

where

$$\bar{\Gamma} = \begin{bmatrix} \bar{\Xi}_{11} & \bar{\Xi}_{12} & -\bar{\mathcal{G}}_{12} & \bar{\Xi}_{14} & -(L\mathfrak{X}_{\{0\}}Q_2)^{\top} & -\mathcal{D} \\ \star & 2\bar{\mathcal{R}} - \bar{\mathcal{G}}_{12} - \bar{\mathcal{G}}_{12}^{\top} & -\bar{\mathcal{R}} + \bar{\mathcal{G}}_{12} & -\eta\,(\mathfrak{X}_{\{1\}}Q_1)^{\top} & 0 & 0 \\ \star & \star & \bar{\mathcal{R}} + \bar{\mathcal{G}} & 0 & 0 & 0 \\ \star & \star & \star & \bar{\Xi}_{44} & 0 & -\eta\mathcal{D} \\ \star & \star & \star & \star & I_q & 0 \\ \star & \star & \star & \star & \star & \gamma I_p \end{bmatrix},$$

$$\bar{\Xi}_{11} = \bar{\mathcal{P}} - \bar{\mathcal{G}} + (1-\bar{d}^2)\bar{\mathcal{R}} - \mathfrak{X}_{\{1\}}H_K \begin{bmatrix} 0 \\ I_{n+q} \end{bmatrix} \bar{\mathcal{P}}_2 - \left(\mathfrak{X}_{\{1\}}H_K \begin{bmatrix} 0 \\ I_{n+q} \end{bmatrix} \bar{\mathcal{P}}_2\right)^\top,$$

$$\bar{\Xi}_{12} = -\bar{\mathcal{R}} + \bar{\mathcal{G}}_{12} - \mathfrak{X}_{\{1\}}H_K \begin{bmatrix} I_{n+q} \\ 0 \end{bmatrix} \bar{\mathcal{P}}_2,$$

$$\bar{\Xi}_{14} = \bar{d}^2\bar{\mathcal{R}} + \bar{\mathcal{P}}_2 - \eta\left(\mathfrak{X}_{\{1\}}H_K \begin{bmatrix} 0 \\ I_{n+q} \end{bmatrix} \bar{\mathcal{P}}_2\right)^\top,$$

$$\bar{\Xi}_{44} = -\bar{\mathcal{P}} - \bar{d}^2\bar{\mathcal{R}} + \eta\left(\bar{\mathcal{P}}_2 + \bar{\mathcal{P}}_2^\top\right),$$

with

$$\mathcal{U}_{d,\{0\}}\mathcal{Q}_2 = 0, \quad \mathfrak{X}_{\{0\}}\mathcal{Q}_1 = 0,$$

and

$$\mathcal{K} = \mathcal{U}_{d,\{0\}}\mathcal{Q}_1 \left(\mathfrak{X}_{\{0\}}\mathcal{Q}_2\right)^{-1},$$

then, for the delay $d(s) \in [0, \bar{d}]$, system (2.7) *is asymptotically stable for $\mathcal{W}(s) = 0$ and achieves an L_2-gain below γ for $\mathcal{W}(s) \neq 0$.*

Proof. Inspired by the procedure of [24], we choose the following Lyapunov-Krasovskii functional:

$$V(s) = V_{\mathcal{P}}(s) + V_{\mathcal{G}}(s) + V_{\mathcal{R}}(s), \tag{3.3}$$

with

$$V_{\mathcal{P}}(s) = \mathfrak{X}^\top(s)\mathcal{P}\mathfrak{X}(s),$$

$$V_{\mathcal{G}}(s) = \sum_{j=s-\bar{d}}^{s-1} \mathfrak{X}^\top(j)\mathcal{G}\mathfrak{X}(j),$$

$$V_{\mathcal{R}}(s) = \bar{d}\sum_{m=-\bar{d}}^{-1}\sum_{j=s+m}^{s-1} \xi^\top(j)\mathcal{R}\xi(j),$$

where $\xi(j) = \mathfrak{X}(j+1) - \mathfrak{X}(j)$ and $\mathcal{P} > 0, \mathcal{G} > 0, \mathcal{R} > 0$ are matrix variables which belong to $\mathbb{R}^{(n+q)\times(n+q)}$. By calculating $V(s+1) - V(s)$, the difference equations can be expressed as follows:

$$V_{\mathcal{P}}(s+1) - V_{\mathcal{P}}(s) = \mathfrak{X}^\top(s+1)\mathcal{P}\mathfrak{X}(s+1) - \mathfrak{X}^\top(s)\mathcal{P}\mathfrak{X}(s),$$

$$V_{\mathcal{G}}(s+1) - V_{\mathcal{G}}(s) = \mathfrak{X}^\top(s)\mathcal{G}\mathfrak{X}(s) - \mathfrak{X}_{\bar{d}}^\top(s)\mathcal{G}\mathfrak{X}_{\bar{d}}(s),$$

$$V_{\mathcal{R}}(s+1) - V_{\mathcal{R}}(s) = \bar{d}^2\xi^\top(s)\mathcal{R}\xi(s) - \bar{d}\sum_{j=s-\bar{d}}^{s-1} \xi^\top(j)\mathcal{R}\xi(j).$$

Break down the following summation formula into two parts

$$\bar{d}\sum_{j=s-\bar{d}}^{s-1} \xi^\top(j)\mathcal{R}\xi(j) = \bar{d}\sum_{j=s-\bar{d}}^{s-1-d(s)} \xi^\top(j)\mathcal{R}\xi(j) + \bar{d}\sum_{j=s-d(s)}^{s-1} \xi^\top(j)\mathcal{R}\xi(j). \tag{3.4}$$

Applying Jensen's inequality and the complementary convex method [24], we obtain

$$\begin{aligned}\bar{d}\sum_{j=s-\bar{d}}^{s-1}\xi^\top(j)\mathcal{R}\xi(j) \geq & \frac{\bar{d}}{\bar{d}-d(s)}\left[\mathfrak{X}_{d(s)}(s)-\mathfrak{X}_{\bar{d}}(s)\right]^\top\mathcal{R}\left[\mathfrak{X}_{d(s)}(s)-\mathfrak{X}_{\bar{d}}(s)\right] \\ & + \frac{\bar{d}}{d(s)}\left[\mathfrak{X}(s)-\mathfrak{X}_{d(s)}(s)\right]^\top\mathcal{R}\left[\mathfrak{X}(s)-\mathfrak{X}_{d(s)}(s)\right] \\ \geq & \begin{bmatrix}\mathfrak{X}(s)-\mathfrak{X}_{d(s)}(s)\\ \mathfrak{X}_{d(s)}(s)-\mathfrak{X}_{\bar{d}}(s)\end{bmatrix}^\top\begin{bmatrix}\mathcal{R} & \mathcal{G}_{12}\\ \star & \mathcal{R}\end{bmatrix}\begin{bmatrix}\mathfrak{X}(s)-\mathfrak{X}_{d(s)}(s)\\ \mathfrak{X}_{d(s)}(s)-\mathfrak{X}_{\bar{d}}(s)\end{bmatrix}\end{aligned} \tag{3.5}$$

Remark 4. *When $d(s) = 0$, the bracketed term $\mathfrak{X}(s) - \mathfrak{X}_{d(s)}(s) = \mathfrak{X}(s) - \mathfrak{X}(s) = 0$ is identically zero, not merely a limiting value. Although the denominator $d(s)$ is also zero, the ratio term $\frac{\bar{d}}{d(s)}\left[\mathfrak{X}(s)-\mathfrak{X}_{d(s)}(s)\right]^\top\mathcal{R}\left[\mathfrak{X}(s)-\mathfrak{X}_{d(s)}(s)\right]$ is by convention taken to be zero, consistent with the original sum over an empty index set. Similarly, when $d(s) = \bar{d}$, the bracketed term $\mathfrak{X}_{d(s)}(s) - \mathfrak{X}_{\bar{d}}(s)$ is identically zero, and the corresponding ratio term is taken to be zero by the same convention. Therefore, inequality (3.5) remains valid for all $d(s) \in \{0, 1, \ldots, \bar{d}\}$ without requiring separate treatment of the boundary cases.*

for any $\mathcal{G}_{12} \in \mathbb{R}^{(n+q)\times(n+q)}$ satisfying

$$\begin{bmatrix}\mathcal{R} & \mathcal{G}_{12}\\ \star & \mathcal{R}\end{bmatrix} \geq 0. \tag{3.6}$$

Assume that

$$\chi^\top(s) = \left[\mathfrak{X}^\top(s), \mathfrak{X}^\top_{d(s)}(s), \mathfrak{X}^\top_{\bar{d}}(s), \mathfrak{X}^\top_{s+1}(s+1)\right]. \tag{3.7}$$

Using (3.5) and (3.7), we obtain

$$V_{\mathcal{R}}(s+1) - V_{\mathcal{R}}(s) \leq \bar{d}^2\xi^\top(s)\mathcal{R}\xi(s) - \chi^\top(s)\Xi_1\chi(s), \tag{3.8}$$

where

$$\Xi_1 = \begin{bmatrix}\mathcal{R} & -\mathcal{R}+\mathcal{G}_{12} & -\mathcal{G}_{12} & 0\\ \star & 2\mathcal{R}-\mathcal{G}_{12}-\mathcal{G}_{12}^\top & -\mathcal{R}+\mathcal{G}_{12} & 0\\ \star & \star & \mathcal{R} & 0\\ \star & \star & \star & 0\end{bmatrix}. \tag{3.9}$$

Now, considering (2.12) and (2.13), we have

$$\mathcal{B}\mathcal{K} = \mathfrak{X}_{\{1\}}H_K\begin{bmatrix}I_n & 0\end{bmatrix}^\top,$$
$$\mathcal{A} = \mathfrak{X}_{\{1\}}H_K\begin{bmatrix}0 & I_{n+q}\end{bmatrix}^\top,$$

subject to

$$0 = \mathcal{U}_{d,\{0\}}H_K\begin{bmatrix}0 & I_n\end{bmatrix}^\top,$$
$$0 = \mathfrak{X}_{\{0\}}H_K\begin{bmatrix}I_n & 0\end{bmatrix}^\top.$$

Using the descriptor method [24], for matrix variables $\mathcal{P}_2, \mathcal{P}_3 \in \mathbb{R}^{(n+q)\times(n+q)}$, we can obtain

$$0 = \varphi_1 + \varphi_2 + \varphi_3, \tag{3.10}$$

where

$$\begin{aligned}
\varphi_1 &= -2\mathfrak{X}^\top(s)\mathcal{P}_2^\top\mathfrak{X}(s+1),\\
\varphi_2 &= -2\mathfrak{X}^\top(s+1)\mathcal{P}_3^\top\mathfrak{X}(s+1),\\
\varphi_3 &= 2\left(\mathfrak{X}^\top(s)\mathcal{P}_2^\top + \mathfrak{X}^\top(s+1)\mathcal{P}_3^\top\right)\mathfrak{X}_{\{1\}}H_K \times \left(\begin{bmatrix} I_{n+q} \\ 0 \end{bmatrix}\mathfrak{X}_{d(s)}(s) + \begin{bmatrix} 0 \\ I_{n+q} \end{bmatrix}\mathfrak{X}(s)\right).
\end{aligned}$$

Then, we rewrite (3.10) in a quadratic form as

$$0 = \chi^\top(s)\Xi_2\chi(s), \tag{3.11}$$

where

$$\Xi_2 = \begin{bmatrix} \Xi_{2,11} & \mathcal{P}_2^\top\mathfrak{X}_{\{1\}}H_K\left(\begin{smallmatrix} I_n \\ 0 \end{smallmatrix}\right) & 0 & -\mathcal{P}_2^\top + \left(\mathcal{P}_3^\top\mathfrak{X}_{\{1\}}H_K\left(\begin{smallmatrix} 0 \\ I_n \end{smallmatrix}\right)\right)^\top \\ \star & 0 & 0 & \left(\mathcal{P}_3^\top\mathfrak{X}_{\{1\}}H_K\left(\begin{smallmatrix} I_n \\ 0 \end{smallmatrix}\right)\right)^\top \\ \star & \star & 0 & 0 \\ \star & \star & \star & -\left(\mathcal{P}_3 + \mathcal{P}_3^\top\right) \end{bmatrix}, \tag{3.12}$$

$$\Xi_{2,11} = \mathcal{P}_2^\top\mathfrak{X}_{\{1\}}H_K\begin{bmatrix} 0 \\ I_{n+q} \end{bmatrix} + \left(\mathcal{P}_2^\top\mathfrak{X}_{\{1\}}H_K\begin{bmatrix} 0 \\ I_{n+q} \end{bmatrix}\right)^\top.$$

Now, considering (3.8), (3.11), and incorporating Ξ_1 and Ξ_2, we derive

$$V(s+1) - V(s) \leq -\chi^\top(s)\Xi\chi(s), \tag{3.13}$$

where

$$\Xi = \begin{bmatrix} \Xi_{11} & \Xi_{12} & -\mathcal{G}_{12} & \Xi_{14} \\ \star & 2\mathcal{R} - \mathcal{G}_{12} - \mathcal{G}_{12}^\top & -\mathcal{R} + \mathcal{G}_{12} & -\left(\mathcal{P}_3^\top\mathfrak{X}_{\{1\}}H_K\left(\begin{smallmatrix} I_{n+q} \\ 0 \end{smallmatrix}\right)\right)^\top \\ \star & \star & \mathcal{R} + \mathcal{G} & 0 \\ \star & \star & \star & \Xi_{44} \end{bmatrix}, \tag{3.14}$$

$$\begin{aligned}
\Xi_{11} &= \mathcal{P} - \mathcal{G} + (1 - \bar{d}^2)\mathcal{R} - \mathcal{P}_2^\top\mathfrak{X}_{\{1\}}H_K\begin{bmatrix} 0 \\ I_{n+q} \end{bmatrix} - \left(\mathcal{P}_2^\top\mathfrak{X}_{\{1\}}H_K\begin{bmatrix} 0 \\ I_{n+q} \end{bmatrix}\right)^\top,\\
\Xi_{12} &= -\mathcal{R} + \mathcal{G}_{12} - \mathcal{P}_2^\top\mathfrak{X}_{\{1\}}H_K\begin{bmatrix} I_{n+q} \\ 0 \end{bmatrix},\\
\Xi_{14} &= \bar{d}^2\mathcal{R} + \mathcal{P}_2^\top - \left(\mathcal{P}_3^\top\mathfrak{X}_{\{1\}}H_K\begin{bmatrix} 0 \\ I_{n+q} \end{bmatrix}\right)^\top,\\
\Xi_{44} &= -\mathcal{P} - \bar{d}^2\mathcal{R} + (\mathcal{P}_3 + \mathcal{P}_3^\top).
\end{aligned}$$

The model exhibits a linear relationship for all decision variables. We set $\mathcal{P}_3 = \eta\mathcal{P}_2$ and $\bar{\mathcal{P}}_2 = \mathcal{P}_2^{-1}$. Through [25], auxiliary matrix variables are introduced

$$\begin{aligned}
Q_1 &= H_K\begin{bmatrix} I_{n+q} \\ 0 \end{bmatrix}\bar{\mathcal{P}}_2,\\
Q_2 &= H_K\begin{bmatrix} 0 \\ I_{n+q} \end{bmatrix}\bar{\mathcal{P}}_2.
\end{aligned} \tag{3.15}$$

Considering (2.9) and (2.13), we have

$$
\begin{aligned}
\mathcal{K}\bar{\mathcal{P}}_2 &= \mathcal{U}_{d,\{0\}}H_K\begin{bmatrix} I_{n+q} \\ 0 \end{bmatrix}\bar{\mathcal{P}}_2 = \mathcal{U}_{d,\{0\}}Q_1, \\
\bar{\mathcal{P}}_2 &= \mathfrak{X}_{\{0\}}H_K\begin{bmatrix} 0 \\ I_{n+q} \end{bmatrix}\bar{\mathcal{P}}_2 = \mathfrak{X}_{\{0\}}Q_2.
\end{aligned} \tag{3.16}
$$

For the performance index,

$$
J_\infty = \sum_{s=0}^{\infty}\left(Z(s)^\top Z(s) - \gamma\mathcal{W}(s)^\top\mathcal{W}(s)\right). \tag{3.17}
$$

If there exists a feedback gain $\mathcal{K}$ to make $J_\infty < 0$, then it can be said that the system achieves an L_2-gain below γ [24]. In order to obtain the gain, we set:

$$
\hat{\chi}^\top(s) = [\chi^\top(s), Z(s)^\top(s), \mathcal{W}(s)^\top]. \tag{3.18}
$$

In this condition, the following inequality should hold:

$$
-\hat{\chi}^\top(s)\Gamma\hat{\chi}(s) \geq V(s+1) - V(s) + \left(Z(s)^\top Z(s) - \gamma\mathcal{W}(s)^\top\mathcal{W}(s)\right), \tag{3.19}
$$

with

$$
\Gamma = \begin{bmatrix} \Theta & \kappa^\top \\ \star & \mathcal{I} \end{bmatrix} > 0, \tag{3.20}
$$

$$
\Theta = \begin{bmatrix} \Xi_{11} & \Xi_{12} & -\mathcal{G}_{12} & \Xi_{14} \\ \star & 2\mathcal{R} - \mathcal{G}_{12} - \mathcal{G}_{12}^\top & -\mathcal{R} + \mathcal{G}_{12} & -\left(\mathcal{P}_3^\top\mathfrak{X}_{\{1\}}H_K\left(\begin{smallmatrix} I_{n+q} \\ 0 \end{smallmatrix}\right)\right)^\top \\ \star & \star & \mathcal{R} + \mathcal{G} & 0 \\ \star & \star & \star & \Xi_{44} \end{bmatrix}, \tag{3.21}
$$

$$
\kappa = \begin{bmatrix} -L & 0 & 0 & 0 \\ -\mathcal{D}^\top\mathcal{P}_2 & 0 & 0 & -\eta\mathcal{D}^\top\mathcal{P}_2 \end{bmatrix}, \mathcal{I} = \begin{bmatrix} I_q & 0 \\ 0 & \gamma I_p \end{bmatrix}. \tag{3.22}
$$

We introduce the congruent transformation $\bar{\Gamma} = \mathbf{P}^\top\Gamma\mathbf{P}$ with

$$
\mathbf{P} = \operatorname{diag}\left(\bar{\mathcal{P}}_2, \bar{\mathcal{P}}_2, \bar{\mathcal{P}}_2, \bar{\mathcal{P}}_2, I_q, I_p\right). \tag{3.23}
$$

It is easy to see that (3.1) can ensure (3.19) holds.

Remark 5. *Compared with reinforcement-learning-based [3, 11] and model-predictive-control-based [5, 7] data-driven methods, the proposed method does not require online iterative learning or repeated online optimization. Instead, it requires only an offline semidefinite program, while the online implementation consists of a simple linear feedback computation. The number of decision variables scales polynomially with the state dimension and the sample size, allowing standard interior-point solvers to efficiently handle problems of practical size. Once the controller gain is computed offline, the online control law requires only a simple matrix multiplication at each sampling instant. Therefore, the computational burden is low, and the proposed method is suitable for real-time control applications.*

Remark 6. *Compared with classic model-based H_∞ approaches [20, 21], the proposed method designs the controller entirely from sampled data without requiring explicit knowledge of the system matrices A and B. In the microgrid scenario studied in this paper, accurately obtaining these matrices requires detailed knowledge of the grid topology and line impedances, which are often difficult to obtain accurately in practice. Even when an approximate model is obtained through system identification, model inaccuracies weaken the robustness guarantees of model-based methods. This further highlights the practical advantage of the proposed data-driven approach.*

4. Simulation results

In this section, the effectiveness of the control design method is verified through a numerical example of a DC microgrid [26]. First, an average model of the islanded operation state of a DC microgrid consisting of two distributed power generation units is established, as shown in Figure 1.

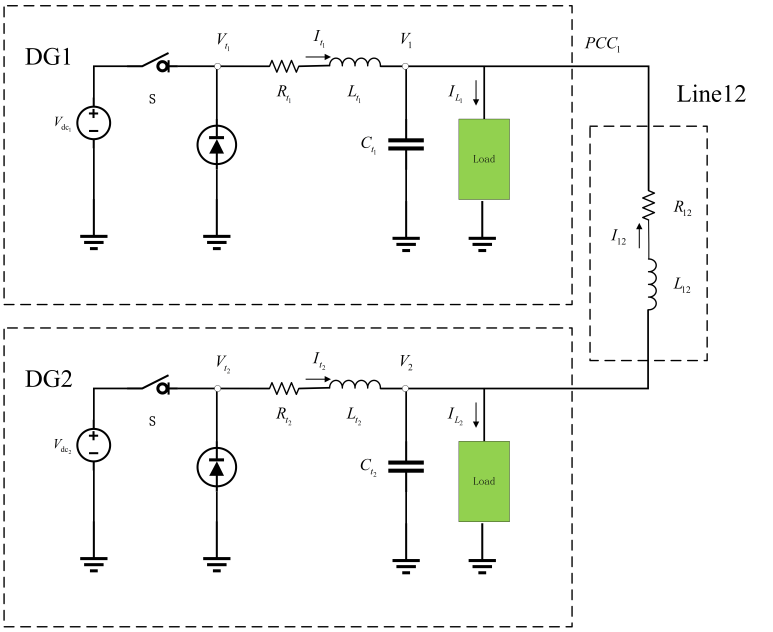

Figure 1. Island DC microgrid model.

Using the quasi-stationary lines approximated model [27]

$$
\begin{aligned}
\frac{dV_1}{dt} &= \frac{1}{C_{t_1}} I_{t_1} - \frac{1}{C_{t_1}} I_{L_1} + \frac{1}{C_{t_1} R_{12}} V_2 - \frac{1}{C_{t_1} R_{12}} V_1, \\
\frac{dI_{t_1}}{dt} &= -\frac{1}{L_{t_1}} V_1 - \frac{R_{t_1}}{L_{t_1}} I_{t_1} + \frac{d_{\text{buck}_1}}{L_{t_1}} V_{dc_1}, \\
\frac{dV_2}{dt} &= \frac{1}{C_{t_2}} I_{t_2} - \frac{1}{C_{t_2}} I_{L_2} + \frac{1}{C_{t_2} R_{12}} V_j - \frac{2}{C_{t_2} R_{12}} V_2, \\
\frac{dI_{t_2}}{dt} &= -\frac{1}{L_{t_2}} V_2 - \frac{R_{t_2}}{L_{t_2}} I_{t_2} + \frac{d_{\text{buck}_2}}{L_{t_2}} V_{dc_2}.
\end{aligned}
$$

Table 2. Parameters of DG.

DGs	V_{ref} (V)	R_t (Ω)	C_t (mF)	L_t (mH)	R_L (Ω)	R_{12} (Ω)	L_{12} (Ω)
DG 1	46	0.2	2.2	1.8	10	0.05	2.1
DG 2	49	0.3	1.9	2.0	6	0.05	2.1

The parameters are shown in Table 2. Therefore, the TDS can be described as follows:

$$\begin{cases} \dot{x}(t) = A_1 x(t) + B_1 u_{d(t)}(t) + D_1 w(t) \\ y(t) = C_1 x(t), \end{cases}$$

where $x(t) = \begin{bmatrix} V_1 & I_{t_1} & V_2 & I_{t_2} \end{bmatrix}^T$, $u(t) = \begin{bmatrix} d_{buck1} V_{dc1} & d_{buck2} V_{dc2} \end{bmatrix}^T$, $w(t) = \begin{bmatrix} I_{L_1} & I_{L_2} \end{bmatrix}^T$, and $y(t) = \begin{bmatrix} V_1 & V_2 \end{bmatrix}^T$,

$$A_1 = \begin{bmatrix} -\frac{1}{C_{t_1} R_{12}} & \frac{1}{C_{t_1}} & \frac{1}{C_{t_1} R_{12}} & 0 \\ -\frac{1}{L_{t_1}} & -\frac{R_{t_1}}{L_{t_1}} & 0 & 0 \\ \frac{1}{C_{t_2} R_{12}} & 0 & -\frac{1}{C_{t_2} R_{12}} & \frac{1}{C_{t_2}} \\ 0 & 0 & -\frac{1}{L_{t_2}} & -\frac{R_{t_2}}{L_{t_2}} \end{bmatrix}, \quad B_1 = \begin{bmatrix} 0 & 0 \\ \frac{1}{L_{t_1}} & 0 \\ 0 & 0 \\ 0 & \frac{1}{L_{t_2}} \end{bmatrix},$$

$$D_1 = \begin{bmatrix} -\frac{1}{C_{t_1}} & 0 \\ 0 & 0 \\ 0 & -\frac{1}{C_{t_2}} \\ 0 & 0 \end{bmatrix}, \quad C_1 = \begin{bmatrix} 1 & 0 & 0 & 0 \\ 0 & 0 & 1 & 0 \end{bmatrix}.$$

By discretizing the continuous system, we can obtain the following LDT-TDS:

$$\begin{cases} x(s+1) = Ax(s) + Bu_{d(s)}(s) + Dw(s) \\ \quad y(s) = Cx(s). \end{cases}$$

In practical applications, the line-to-ground capacitance C_t can be roughly measured. However, the rest of the power grid structure is complex, making it difficult to obtain an accurate network structure model. The approximate network structure model therefore has significant errors. Therefore, we assume that matrices A and B are unknown but D is known.

In the microgrid scenario studied in this paper, model-based methods face a practical difficulty, since accurately obtaining the system matrices A and B requires detailed knowledge of the grid topology, line impedances, and the switching characteristics of power converters. These parameters are often difficult to measure accurately or vary with operating conditions in practice. This limits the reliability of model-based time-varying delay control methods in such scenarios. This is the practical motivation behind the data-driven approach adopted in this paper, where the controller is designed solely from sampled data rather than an explicit system model.

If the actual value of the disturbance matrix D deviates from its assumed nominal value, this parameter uncertainty manifests as an additional, unmodeled disturbance entering the closed-loop disturbance channel. The proposed controller is designed within the H_∞ framework and possesses a certain degree of robustness against disturbances. A small deviation in D is therefore expected to cause only a moderate degradation in tracking performance without affecting closed-loop stability.

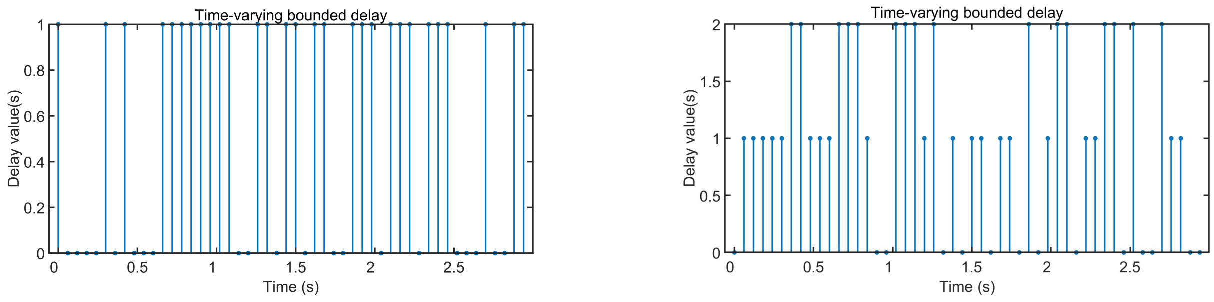

(a) $\bar{d} = 1$ **(b)** $\bar{d} = 2$

Figure 2. Time-varying bounded delay sequences used in the two test cases.

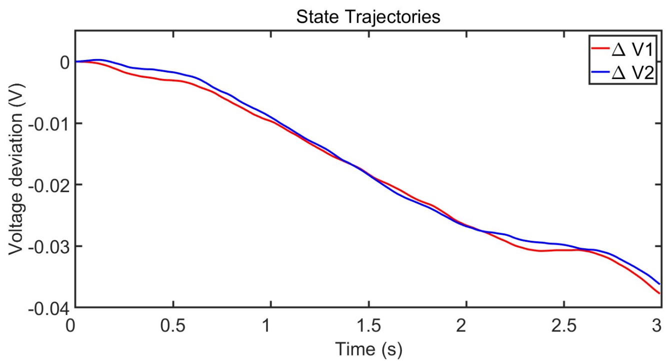

Figure 3. Voltage deviation before control.

The simulation parameters are set as follows: the tuning parameter is $\eta = 3$, and the disturbance attenuation level is $\gamma = 1$. A total of $K = 100$ samples are collected under open-loop conditions with a persistently exciting input signal. The collected data matrix is verified to satisfy $\text{rank}(W_0) = 8$, which equals $m + n + q$, where $m = 2$, $n = 4$, and $q = 2$, confirming the validity of the data-driven approach. The collected data is assumed to be free of measurement noise but inherently include the disturbance and the time-varying delay present during data collection. This is consistent with the H_∞ robust control framework adopted in this paper, which does not require noise-free measurements. The value of $\eta = 3$ is selected after a preliminary search over $\{1, 2, 3, 5\}$, with little effect on the results.

To verify the feasibility of the controller, the simulations are conducted in a discrete-time simulation environment. The sampling interval is set to $0.01s$. We assume the control input has time-varying bounded delays, whose delay sequences for the two test cases are shown in Figure 2. Before the designed controller is involved in control, simulation data collection is performed. Due to the presence of delay and interference, the voltage error cannot approach 0, and the system is in an unstable state, as shown in Figure 3. We can collect the state and input data under this condition as the basis for designing the controller.

To examine the effect of the delay upper bound on the closed-loop performance, the controller is tested under two cases, $\bar{d} = 1$ and $\bar{d} = 2$. These two values are chosen with reference to the range of delay magnitudes observed in the practical scenario. The same random seed is used to generate the data collection, delay, and disturbance realizations in both cases, ensuring that the comparison reflects the effect of $\bar{d}$ itself rather than randomness across different runs. As shown in Figure 4, after the controller participates in voltage regulation, the output voltages V_1 and V_2 track their reference values of 46 V and 49 V within approximately 1.3 s in both cases. Table 3 reports the steady-state error, the settling time within a 2% error band, and the overshoot for both outputs under the two cases.

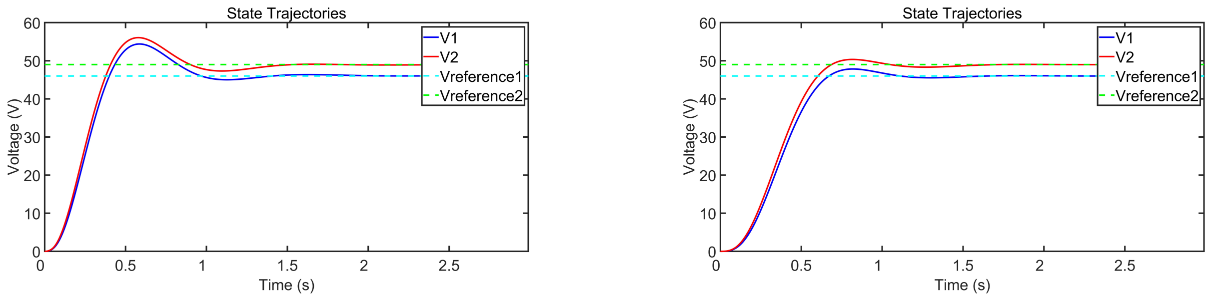

(a) $\bar{d} = 1$ **(b)** $\bar{d} = 2$

Figure 4. Voltage tracking control simulation under two delay upper bounds.

Table 3. Quantitative performance comparison under different delay upper bounds.

	V_1		V_2	
	$\bar{d} = 1$	$\bar{d} = 2$	$\bar{d} = 1$	$\bar{d} = 2$
Steady-state error (V)	0.0253	0.0033	0.0172	0.0010
Settling time (s)	1.180	0.980	1.290	0.930
Overshoot (%)	18.14	3.82	14.32	3.01

The results in Table 3 show that the closed-loop performance under $\bar{d} = 2$ is consistently better than under $\bar{d} = 1$ in terms of steady-state error, settling time, and overshoot. This indicates that, within the range considered, increasing the delay upper bound does not necessarily degrade the closed-loop performance, which may be related to the specific realization of the data used in this example. Future work will conduct a more comprehensive statistical assessment based on multiple independent data collections and delay and disturbance realizations. These results demonstrate that the proposed algorithm is able to maintain set-point tracking in the presence of time-varying bounded delays and unknown disturbances.

Remark 7. *The conservativeness of the linear matrix inequality (LMI) condition in Theorem 1 also increases with the delay bound $\bar{d}$, since the Jensen-type bound used in inequality* (3.5) *becomes looser as $\bar{d}$ grows. This may render the LMI infeasible for sufficiently large $\bar{d}$. For instance, in this example, the LMI in Theorem 1 becomes infeasible when $\bar{d} = 3$, which is consistent with the increasing conservativeness as $\bar{d}$ grows. Employing tighter bounding techniques could reduce this conservativeness and is left for another direction of future work.*

5. Conclusions

This paper primarily investigates data-driven set-point tracking control for systems with input delay and designs a robust controller based on sampled data. The proposed method relies solely on recorded input and state data, without requiring an explicit system model. Robust data-driven control techniques are employed in the design to guarantee the stability of the closed-loop system. Furthermore, the feasibility of the proposed control design is demonstrated through a microgrid application. The results show effective tracking performance without requiring detailed knowledge of the microgrid structural parameters.

It is worth noting that the proposed method has certain limitations. The delay $d(s)$ is assumed to be time-varying but bounded within a known range, without directly addressing scenarios involving an unbounded delay or a delay whose upper bound is itself unknown. This assumption is applicable to many practical scenarios, such as network-induced delays with a known worst-case bound. In addition, the microgrid model is obtained through small-signal linearization rather than capturing the inherently nonlinear dynamics of practical power converters. Extending the proposed framework to handle general delay patterns and nonlinear dynamics remains an important direction for future work.

Use of AI tools declaration

The authors declare they have not used Artificial Intelligence (AI) tools in the creation of this article.

Conflict of interest

The authors declare there is no conflict of interest.

References

1. Z. S. Hou, Z. Wang, From model-based control to data-driven control: Survey, classification and perspective, *Inf. Sci.*, **235** (2013), 3–35. https://doi.org/10.1016/j.ins.2012.07.014
2. Z. S. Hou, S. T. Jin, Data-driven model-free adaptive control for a class of MIMO nonlinear discrete-time systems, *IEEE Trans. Neural Networks*, **22** (2011), 2173–2188. https://doi.org/10.1109/TNN.2011.2176141
3. Y. Wang, K. Zhao, J. L. G. Guirao, K. Pan, H. Chen, Online intelligent maneuvering penetration methods of missile with respect to unknown intercepting strategies based on reinforcement learning, *Electron. Res. Arch.*, **30** (2022), 4366–4381. https://doi.org/10.3934/era.2022221
4. L. Zhang, Vibration analysis and multi-state feedback control of maglev vehicle-guideway coupling system, *Electron. Res. Arch.*, **30** (2022), 3887–3901. https://doi.org/10.3934/era.2022198
5. J. Berberich, J. Köhler, M. A. Müller, F. Allgöwer, Data-driven model predictive control with stability and robustness guarantees, *IEEE Trans. Autom. Control*, **66** (2021), 1702–1717. https://doi.org/10.1109/TAC.2020.3000182
6. P. Yu, S. Tan, J. Guo, Y. Song, Data-driven optimal controller design for sub-satellite deployment of tethered satellite system, *Electron. Res. Arch.*, **32** (2024), 505–522. https://doi.org/10.3934/era.2024025
7. L. Huang, J. Zhen, J. Lygeros, F. Dörfler, Robust data-enabled predictive control: Tractable formulations and performance guarantees, *IEEE Trans. Autom. Control*, **68** (2023), 3163–3170. https://doi.org/10.1109/TAC.2023.3241282

8. M. Wang, J. Qiu, H. Yan, Y. Tian, Z. Li, Data-driven control for discrete-time piecewise affine systems, *Automatica*, **155** (2023), 111168. https://doi.org/10.1016/j.automatica.2023.111168
9. J. G. Rueda-Escobedo, E. Fridman, J. Schiffer, Data-driven control for linear discrete-time delay systems, *IEEE Trans. Autom. Control*, **67** (2022), 3321–3336. https://doi.org/10.1109/TAC.2021.3096896
10. X. Y. Wang, G. D. Wang, S. H. Li, Distributed finite-time optimization for disturbed second-order multiagent systems, *IEEE Trans. Cybern.*, **51** (2021), 4634–4647. https://doi.org/10.1109/TCYB.2020.2988490
11. H. Modares, F. L. Lewis, Z. P. Jiang, H_∞ tracking control of completely unknown continuous-time systems via off-policy reinforcement learning, *IEEE Trans. Neural Networks Learn. Syst.*, **26** (2015), 2550–2562. https://doi.org/10.1109/TNNLS.2015.2441749
12. M. Rotulo, C. De Persis, P. Tesi, Online learning of data-driven controllers for unknown switched linear systems, *Automatica*, **145** (2022), 110519. https://doi.org/10.1016/j.automatica.2022.110519
13. T. Hu, X. Xu, T. M. Nguyen, F. Liu, S. Yuan, L. Xie, Tire wear aware trajectory tracking control for multi-axle swerve-drive autonomous mobile robots, *J. Autom. Intell.*, **4** (2025), 243–253. https://doi.org/10.1016/j.jai.2025.05.003
14. J. X. Zhang, T. Chai, Fault-tolerant control of wheeled mobile robots with prescribed trajectory tracking performance, *J. Autom. Intell.*, **4** (2025), 73–81. https://doi.org/10.1016/j.jai.2025.03.003
15. A. S. Bazanella, L. Campestrini, D. Eckhard, The data-driven approach to classical control theory, *Annu. Rev. Control*, **56** (2023), 100906. https://doi.org/10.1016/j.arcontrol.2023.100906
16. K. J. Åström, P. R. Kumar, Control: A perspective, *Automatica*, **50** (2014), 3–43. https://doi.org/10.1016/j.automatica.2013.10.012
17. Z. Bubnicki, *Modern Control Theory*, Springer Science & Business Media, Berlin, 2005. https://doi.org/10.1007/3-540-28087-1
18. P. J. Antsaklis, A. N. Michel, *Linear Systems*, Birkhäuser, Boston, 2006. https://doi.org/10.1007/0-8176-4435-0
19. Y. Xu, L. Zhou, J. Zhao, L. Ma, C. Yang, Direct data-driven optimal set-point tracking control of linear discrete-time systems, *IEEE Trans. Circuits Syst. II Express Briefs*, **71** (2024), 3795–3799. https://doi.org/10.1109/TCSII.2024.3368271
20. F. Yang, J. He, D. Wang, New stability criteria of delayed load frequency control systems via infinite-series-based inequality, *IEEE Trans. Ind. Inf.*, **14** (2018), 231–240. https://doi.org/10.1109/TII.2017.2751510
21. Z. Jia, X. Li, Q. Cui, L. Li, Asymptotical stability of stochastic delayed time-varying systems with stochastic delayed impulses, *Int. J. Syst. Sci.*, **56** (2025), 1662–1674. https://doi.org/10.1080/00207721.2024.2429024
22. Y. Liu, H. Zhang, R. Yu, Q. Qu, Data-driven optimal tracking control for discrete-time systems with delays using adaptive dynamic programming, *J. Franklin Inst.*, **355** (2018), 5649–5666. https://doi.org/10.1016/j.jfranklin.2018.06.013

23. L. Cui, B. Pang, M. Krstić, Z. Jiang, Learning-based adaptive optimal control of linear time-delay systems: A value iteration approach, *Automatica*, **171** (2025), 111944. https://doi.org/10.1016/j.automatica.2024.111944

24. K. Gu, V. L. Kharitonov, J. Chen, *Introduction to Time-Delay Systems: Analysis and Control*, Springer, Boston, 2014.

25. C. De Persis, P. Tesi, Formulas for data-driven control: Stabilization, optimality, and robustness, *IEEE Trans. Automat. Control*, **65** (2020), 909–924. https://doi.org/10.1109/TAC.2019.2959924

26. S. Derakhshan, M. Shafiee-Rad, Q. Shafiee, M. R. Jahed-Motlagh, S. Sahoo, F. Blaabjerg, Decentralized voltage control of autonomous dc microgrids with robust performance approach, *IEEE J. Emerging Sel. Top. Power Electron.*, **9** (2021), 5508–5520. https://doi.org/10.1109/JESTPE.2021.3054723

27. V. Venkatasubramanian, H. Schattler, J. Zaborszky, Fast time-varying phasor analysis in the balanced three-phase large electric power system, *IEEE Trans. Autom. Control*, **40** (1995), 1975–1982. https://doi.org/10.1109/9.471228